Advanced Composite Materials
Publication details, including instructions for authors and subscription information:
http://www.tandfonline.com/loi/tacm20

Comparison of strength and damage for notched FRP plates made by injection molding with that from machining

Toshihiro Yamamoto & Hiizu Hyakutake

Version of record first published: 02 Apr 2012.

To cite this article: Toshihiro Yamamoto & Hiizu Hyakutake (2002): Comparison of strength and damage for notched FRP plates made by injection molding with that from machining , Advanced Composite Materials, 11:4, 351-363

To link to this article: http://dx.doi.org/10.1163/156855102321669172

Adv. Composite Mater., Vol. 11, No. 4, pp. 351–363 (2003)

Also available online - www.vsppub.com

Comparison of strength and damage for notched FRP plates made by injection molding with that from machining

TOSHIHIRO YAMAMOTO [1,*] and HIIZU HYAKUTAKE [2]

[1] *Faculty of Engineering, Fukuoka University, 8-19-1 Nanakuma, Fukuoaka 814-0180, Japan*
[2] *Department of Mechanical Engineering, Faculty of Engineering, Fukuoka University, Fukuoka 814-0180, Japan*

Received 5 April 2002; accepted 15 January 2003

Abstract—The strength and damage for two kinds of notched specimen have been investigated. We used an injection molded specimen (IM specimen) made by injection molding using a metal mold of a notched specimen, and a machined specimen (M specimen) made from plate by machining. The orientation of the fiber near the notch roots in the IM specimen and the M specimen is slightly different. The investigation was accomplished by obtaining experimental data of the static tension and fatigue tests on the notched plate of a short glass fiber-reinforced polycarbonate. To evaluate the damage near the notch root, we measured the luminance distributions by means of a luminance-measuring system with a CCD camera. The stress concentration and the similarity of stress distribution near the notch root of the IM specimen were compared with those of the M specimen. For the two kinds of specimen, for both of which the maximum elastic stress, σ_{max}, and notch-root radius ρ were equal to each other, the strength and the process of damage initiation were similar under static tension. On the other hand, the number of loading cycles to fatigue damage initiation of the M specimen was fewer than that of the IM specimen.

Keywords: FRP; notch; fatigue; tension; damage; injection molding; machining; luminance.

1. INTRODUCTION

Because of their importance in design applications, the fracture and fatigue of notched FRP specimens have been the subject of much research [1–4]. Such a notch for short fiber reinforced plastics is produced by two methods; injection molding of a notched FRP plate or machining by cutting FRP plates.

The aim of the present research was to investigate the effects of the machining of a notch on the strength and the damage initiation of short fiber reinforced plastics

*To whom correspondence should be addressed. E-mail: yamamott@fukuoka-u.ac.jp

(FRPs). This was accomplished by obtaining experimental data from static tension tests and fatigue tests on the injection molded specimen (IM specimen) made by injection molding using a metal mold of a notched specimen, and a machined specimen (M specimen) made from plate by machining. The M specimen and the IM specimen were made from the same pellets of a short glass fiber-reinforced polycarbonate. However, the orientation of the fiber near the notch root of the IM specimen and the M specimen are slightly but significantly different.

To evaluate the strength and the damage near the notch root, we used a fracture criterion in static load [5] and a fatigue failure criterion [6] for notched FRP plates. The validity of the fracture criterion [5, 7, 8] and the fatigue failure criterion [6, 9, 10] was confirmed previously for notched FRP plates. The criterion is based on the idea of stress concentration and the similarity of stress distribution near the notch root.

For notched FRP plates under static and cyclic loading, the damaged zone initiates and grows near the notch root prior to fracture. To evaluate the damage, we measured successively the luminance distributions by means of a luminance-measuring system with a CCD camera [8–10]. To reveal the process of microcracking, we observed the notch-root surface with a microscope.

2. THEORY

Studying stress distribution near the notch root, Hyakutake *et al.* [5] have obtained a fracture criterion for FRP plates having intermediate notch-root radii in static load. The result of stress analysis near the notch root shows that the stress distributions near the notch root are the same in all specimens for which both the maximum elastic stress, $\sigma_{\max}$, and notch-root radius ρ are equal to each other [5, 6]. In other words, the stress distribution near the notch root is independent of notch depth, notch angle, and so on [5, 6]. Therefore, the severity of stress near the notch root is determined by both the maximum elastic stress $\sigma_{\max}$ and the notch-root radius ρ [5]. It is suggested that the elastoplastic stress distributions near the notch root after small-scale yielding or damage are the same in all specimens, for which both the $\sigma_{\max}$ and ρ are equal in all cases.

On the basis of the similarity of stress distribution near the notch root, the fracture criterion for a notched plate under static load is expressed as [5]

$$\sigma_{\max} = \sigma_{\max,c}(\rho), \tag{1}$$

where $\sigma_{\max}$ is the maximum elastic stress at fracture and is determined as the product of the nominal stress and the geometrical stress concentration factor. The parameter $\sigma_{\max,c}$ is a material constant which is governed by the notch-root radius ρ only and is independent of notch depth and notch angle, and so on.

In addition, the damage near the notch root also seems to be dependent on the severity of stress near the notch root. Under the condition of cyclic loading, it is considered that the initiation of fatigue damage near the notch root is determined by

both the magnitude of the stress and the repetition of loading. The fatigue failure criterion in cyclic loading is expressed as [6]

$$\sigma_{\max} \cdot (N_{\mathrm{d}})^m = C(\rho), \tag{2}$$

where N_{d} is the number of loading cycles to fatigue damage initiation. The parameters m and C are material constants. The interpretation of N_{d} will be discussed later.

As mentioned before, the fracture criterion of equation (1) and the fatigue failure criterion of equation (2) are applicable to several kinds of FRP plate [5–10].

3. EXPERIMENTAL PROCEDURE

The material used was a short glass fiber-reinforced polycarbonate supplied by Idemitsu Petrochemical Co. Two kinds of notched specimen were used: an injection molded specimen (IM specimen) and a machined specimen (M specimen). The IM specimen was made by injection molding using a metal mold of a notched specimen. The M specimen was made from a plate by machining. The dimensions of the plate of the M specimen were 70 mm width, 270 mm length and 3 mm thickness. The plates for the M specimen and for the IM specimen (4 mm thickness) were made from the same pellets of the GFRP by injection molding.

Photomicrographs of a transverse section are shown in Fig. 1. The plate contained 30% E-glass fiber by weight. The length of glass fiber was 1 mm or less. The short aligned fibers for the M specimen were almost in the direction of the length of the plate, which was in the flow direction of the surface layers. In the central layer for the M specimen, the fibers were aligned transverse to the flow direction. However, the central layer was thin (about 0.1 mm). On the other hand, the central layer was not observed for the IM specimen.

Figure 2 shows transmitted light photographs near the notch root. For the IM specimen, the fiber was oriented along the notch root. On the other hand, for the M specimen, the fiber was almost oriented in the principal direction of the specimen. It is evident that the orientation of the fiber near the notch root for the IM specimen is different from that for the M specimen.

The shapes and dimensions of specimens of the notched plate are shown in Fig. 3. The notch-root radius, notch depth and width of specimen are the same in both the IM specimen and the M specimen. The notch-root radius ρ ranged from 0.2 to 10 mm. The notch angle is 90° for the IM specimen and 0° for the M specimen.

Static tension tests were performed by using an Instron-type testing machine at a constant cross-head speed of 0.5 mm/min. Fatigue tests of pulsating tension were made on a servohydraulic material test system at frequency 2 Hz at room temperature.

To evaluate the damage, we measured the luminance distributions near the notch root during static and fatigue testing. The luminance-measuring system with a CCD camera is shown in Fig. 4. The specimen is illuminated from the left side

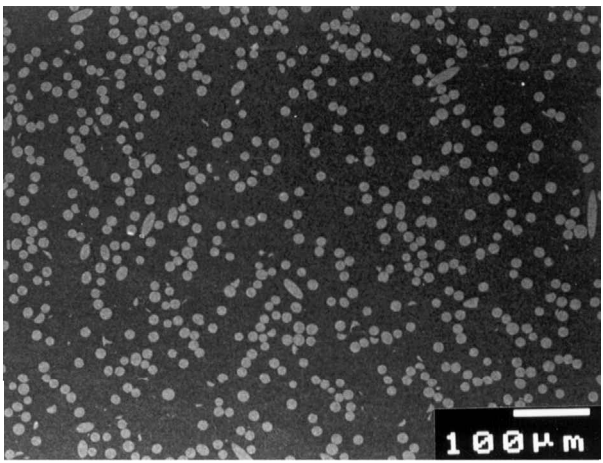

(a)

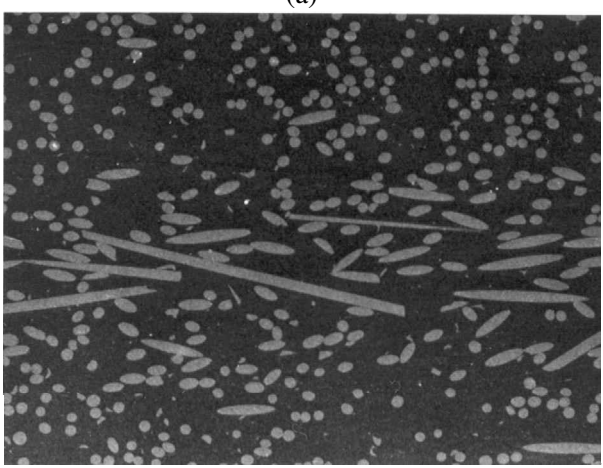

(b)

Figure 1. Photomicrographs showing a transverse section: (a) IM specimen, (b) M specimen.

by an incident light beam during test and the light transmitted through the specimen is received by a CCD camera. The luminance distributions near the notch root are measured by the digital image processor. By means of CCD camera and image processor, we can easily measure the luminance distributions during test and determine the area of damaged zone. It was confirmed previously that the luminance-measuring system was applicable to evaluate the damage of translucent materials such as GFRP plate [8–10].

4. RESULTS AND DISCUSSION

Figure 5 shows the processes of damage initiation and growth near the notch root under static tension. The patterns with light and shade correspond to the value of

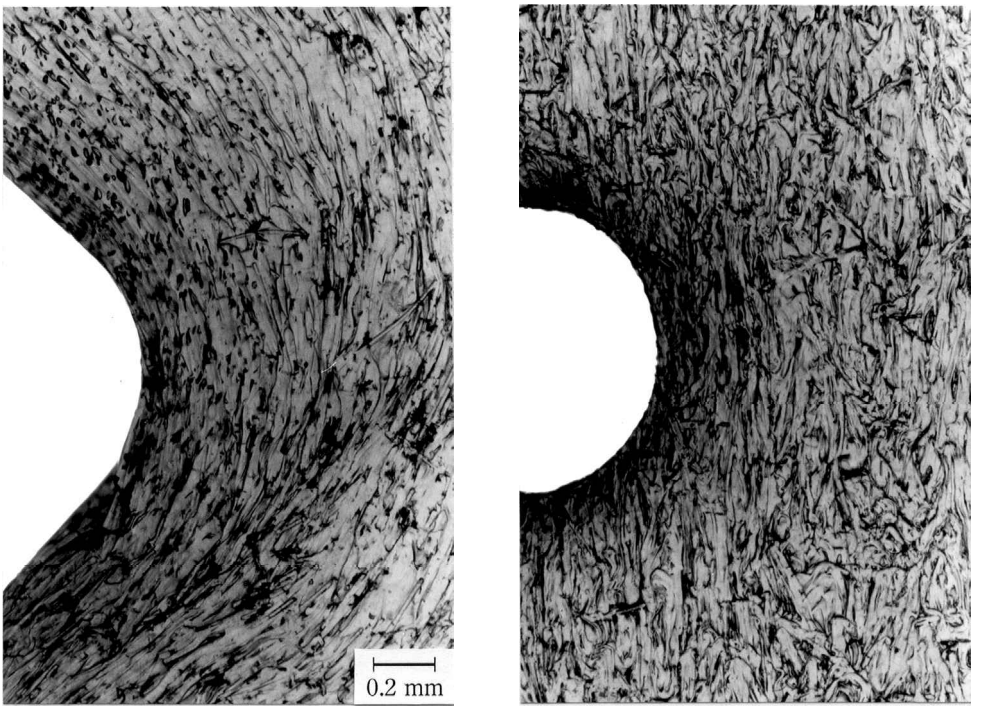

Figure 2. Transmitted light photographs near the notch root ($\rho = 0.5$ mm); (a) IM specimen, (b) M specimen.

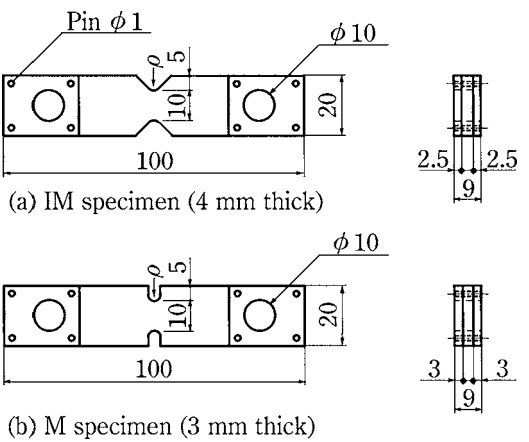

Figure 3. Test-specimen dimensions (mm); (a) IM specimen, (b) M specimen.

relative luminance that was made at four steps, 75, 70, 65 and 60%. The value of relative luminance, R.L. is the ratio of the luminance at a specific stress to the luminance before testing.

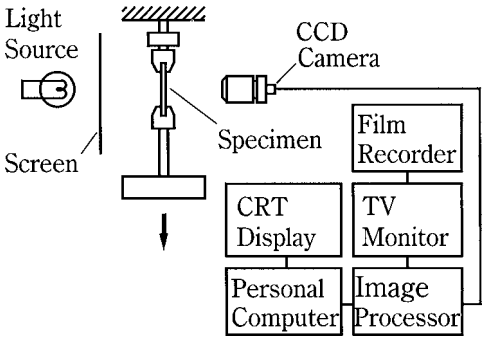

Figure 4. Luminance-measuring system.

The microcracks initiated at the end corner of glass fiber on the notch-root surface [10]. With the increase in the load, the microcracks joined together and the crack expanded to the wide area on the notch-root surface. The decrease of luminance is associated with irreversible microfracture such as microcracks [10]. The damage accumulated severely at the region where the value of relative luminance was small. The processes of damage initiation and growth of the IM specimen under static tension were similar to that of the M specimen, as shown in Fig. 5.

The relation between the area of damaged zone and the maximum elastic stress σ_{max} is represented in Fig. 6. It can be seen that the area of damaged zone has a one-to-one correspondence with a notch-root radius. For the growth curve of the damaged area, there is no difference between the IM specimen and the M specimen under the static tension. The experimental values for which $\rho = 0.5$ mm were scattered. Exact solution to the cause could not be obtained.

Figure 7 shows the maximum elastic stress at fracture in static tension *versus* notch-root radius ρ. As can be seen from Fig. 7, each experimental point of the IM specimen fell in close proximity to the characteristic curve for the M specimen.

Figures 8 and 9 show the process of microcrack growth on the notch-root surface for the IM specimen (Fig. 8) and the M specimen (Fig. 9) in fatigue test. The σ_{max} and ρ are almost same in both specimens. For the IM specimen, microcracks appeared at the end of the glass fiber on the notch-root surface at 2×10^4 cycles, as shown in Fig. 8. Several microcracks joined together and developed into a main crack. At 1.2×10^5 cycles, a main crack on the notch-root surface propagated over the whole plate thickness. Then, the fatigue crack propagated in the width direction of the specimen.

For the M specimen, the glass fiber, which is shorter than that of the IM specimen, is mainly observed as shown in Fig. 9. In other words, the orientation of the glass fiber for the IM specimen is different from that of the M specimen. The process of the initiation and growth of fatigue damage on the notch-root surface for the M specimen are similar to that of the IM specimen. However, the time of initiation of fatigue damage for the M specimen is much earlier than that of the IM specimen. As shown in Fig. 8, the initiation of the microcrack was observed for the IM specimen

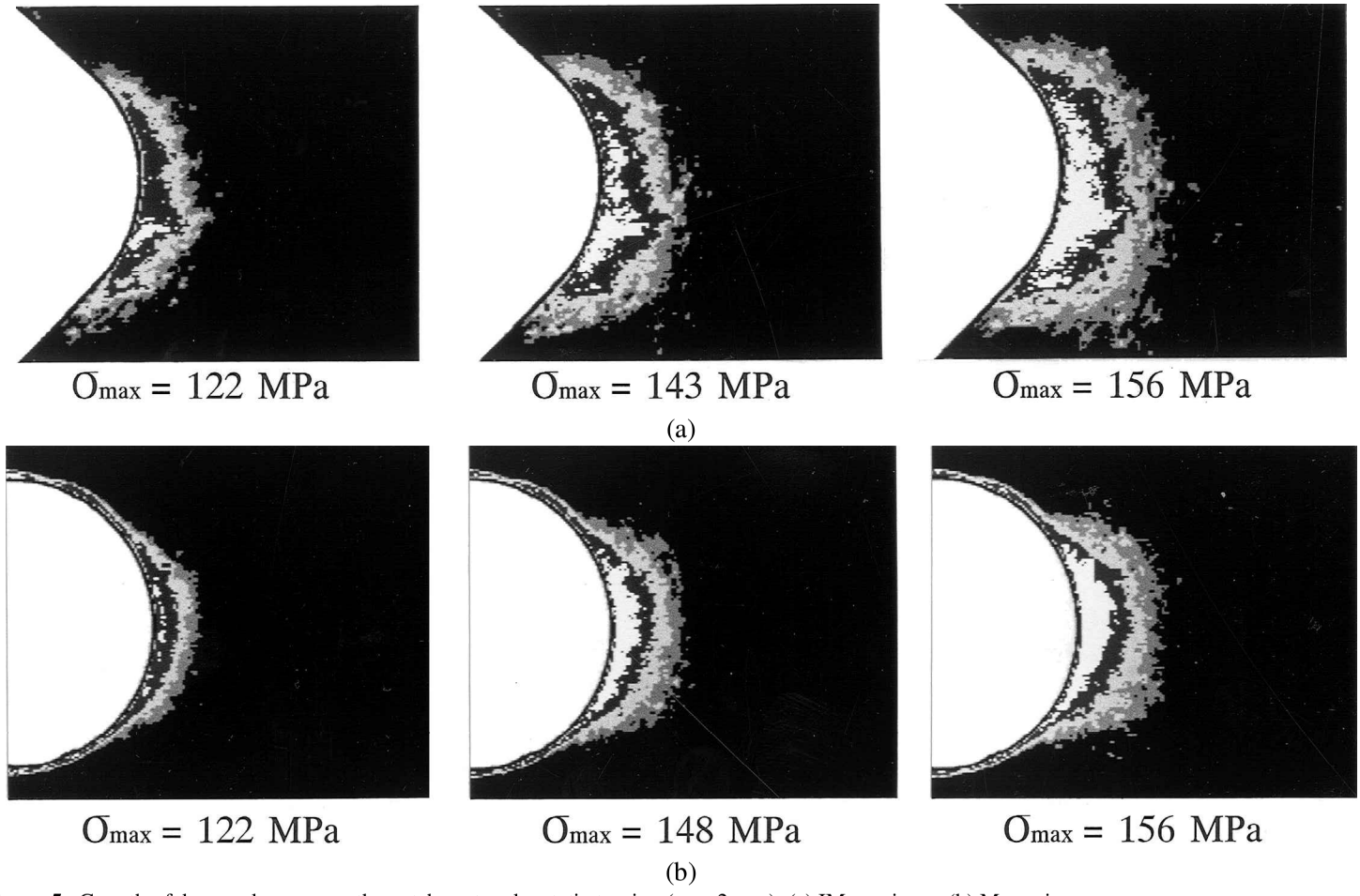

Figure 5. Growth of damaged zone near the notch root under static tension ($\rho = 2$ mm); (a) IM specimen, (b) M specimen.

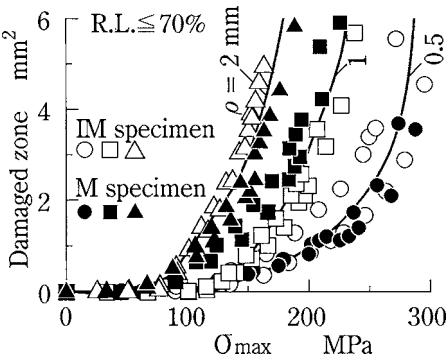

Figure 6. Area of damaged zone *versus* the maximum elastic stress σ_{max} under static tension.

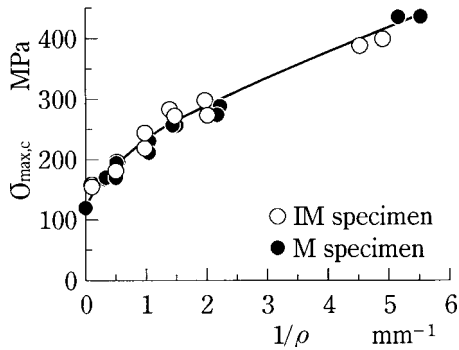

Figure 7. Maximum elastic stress at fracture, $\sigma_{max,c}$ *versus* notch-root radius ρ under static tension.

at 2×10^4 cycles. On the other hand, the microcrack was already initiated and considerably grown for the M specimen at 1.6×10^4 cycles, as can be seen in Fig. 9. For the M specimen, a main crack on the notch-root surface propagated over the whole plate thickness at 4.5×10^4 cycles (Fig. 9).

Figure 10 shows the change of luminance distributions near the notch root for the IM specimen (Fig. 10a) and for the M specimen (Fig. 10b) in fatigue test. The values of σ_{max}, ρ and number of cycles for the two specimens arranged in each file are almost equal. As shown in Fig. 10, the configurations of fatigue-damage zone are different in each file. It can be seen that the processes of fatigue damage initiation and growth of the IM specimen were different from that of the M specimen.

Fatigue damage accumulated severely at the region where R.L. was small, as mentioned before. Figure 11 show the growth curves of the area of fatigue-damage zone where R.L. $\leqslant$ 60% for a constant notch-root radius. The growth curve of fatigue-damage zone for the IM specimen is different from that of the M specimen for the same value of the maximum elastic stress. The fatigue-damage zone increased rapidly over 0.1 mm^2. We determined that N_d is the number of loading cycles at the area of fatigue-damage zone = 0.1 mm^2 [9, 10].

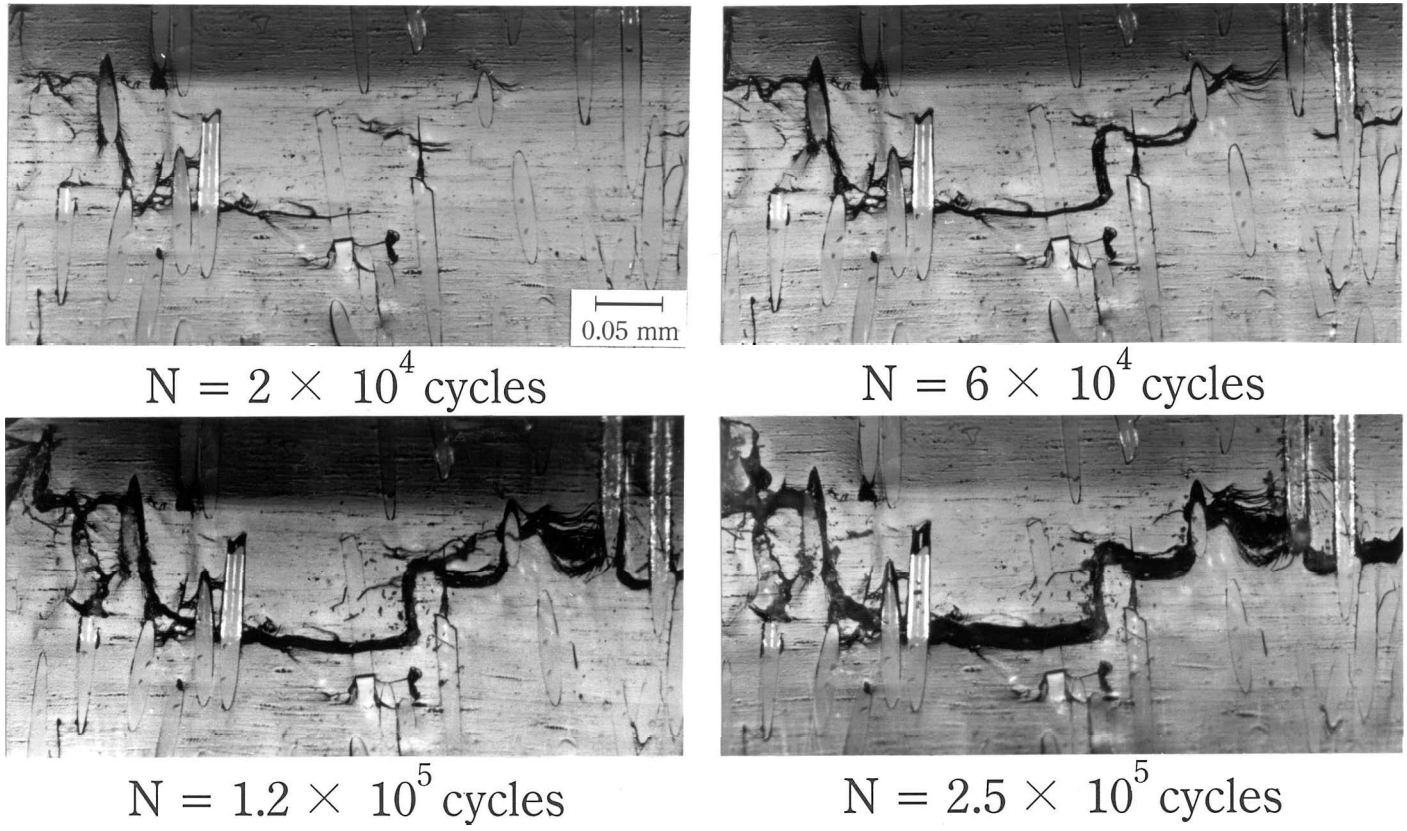

Figure 8. Microcrack growth on the notch-root surface for the IM specimen in fatigue test ($\sigma_{max} = 78$ MPa, $\rho = 1$ mm, $N_f = 2.51 \times 10^5$ cycles).

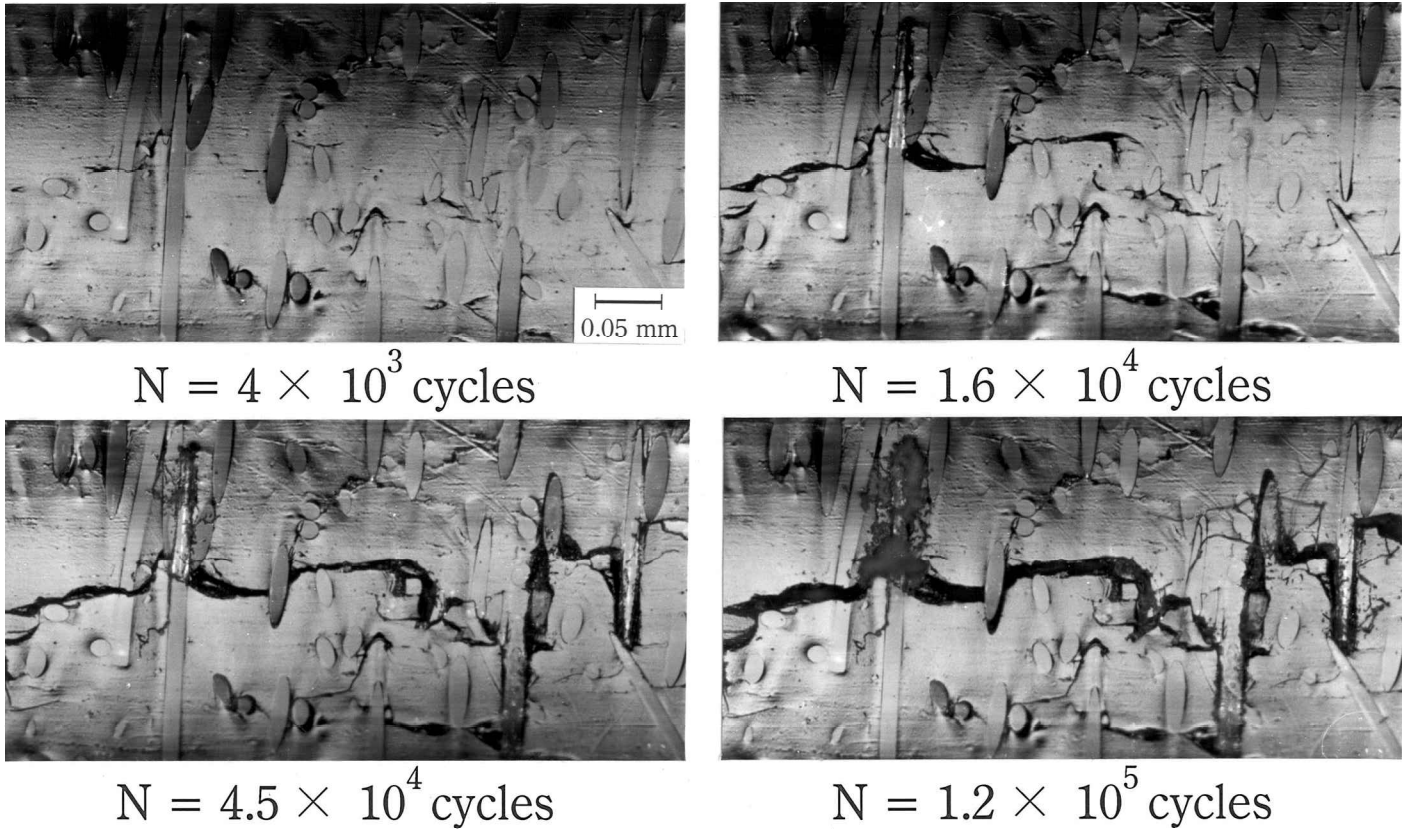

Figure 9. Microcrack growth on the notch-root surface for the M specimen in fatigue test ($\sigma_{max} = 81$ MPa, $\rho = 1$ mm, $N_f = 1.35 \times 10^5$ cycles).

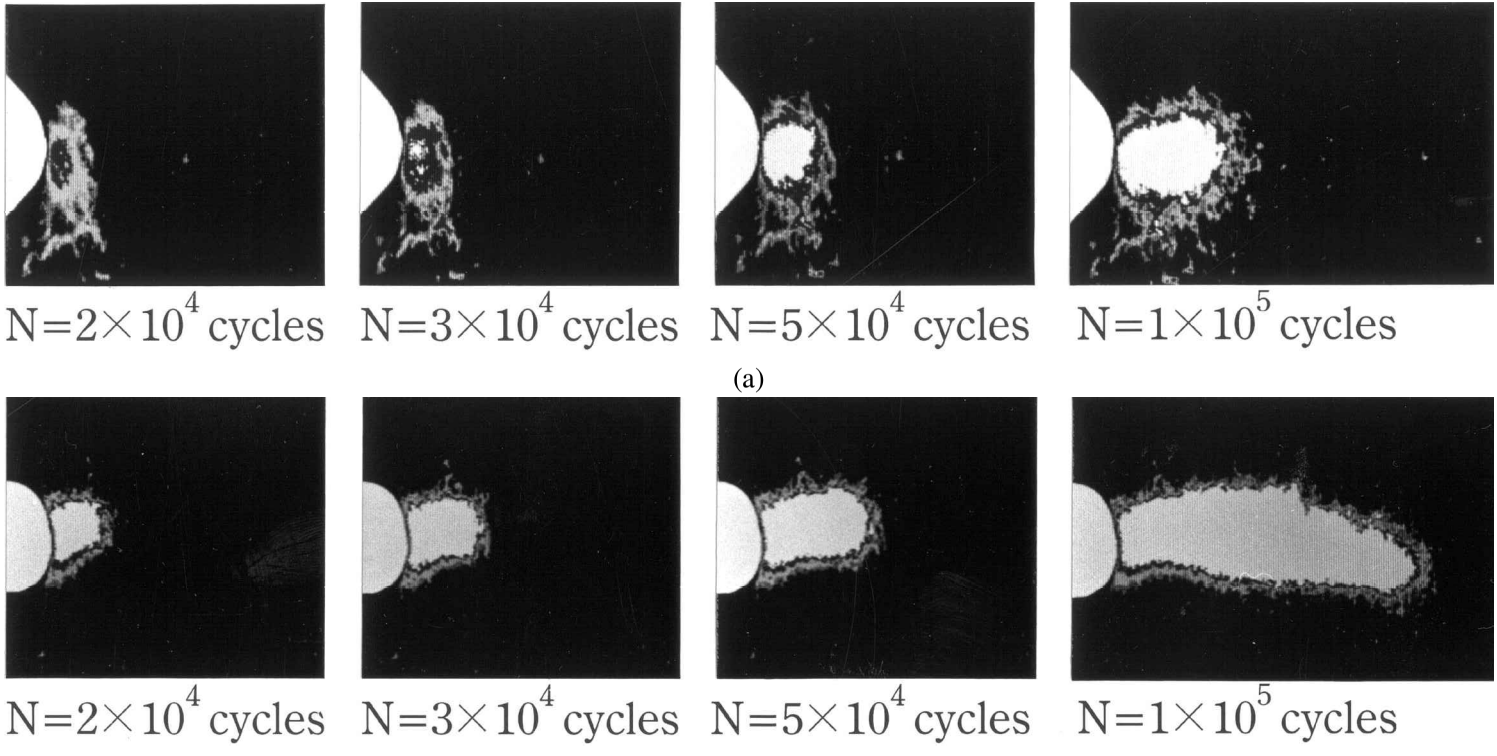

Figure 10. Luminance distributions near the notch root in fatigue test ($\rho = 0.5$ mm); (a) IM specimen, (b) M specimen.

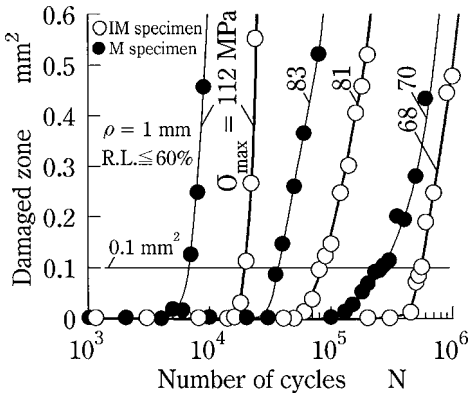

Figure 11. Growth of the area of fatigue-damage zone.

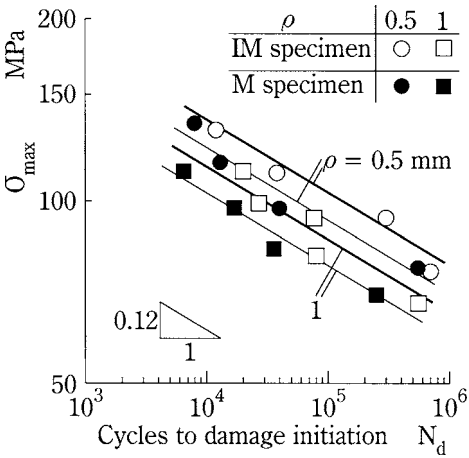

Figure 12. The relation between the maximum elastic stress σ_{max} *versus* the cycles to fatigue damage initiation N_d.

Figure 12 shows the relationship between the maximum elastic stress and the fatigue-damage initiation N_d for a constant notch-root radius ρ. The processes of fatigue damage initiation of the IM specimen were different from that of the M specimen. As can be seen from Fig. 12, the number of loading cycles to fatigue-damage initiation of the M specimen was fewer than that of the IM specimen.

In the fatigue test, if the low stress compared to static load test is repeated, it is considered that the fatigue crack initiated only in the region where the stress concentration was locally high. After the fatigue crack initiated, only the fatigue crack propagated. Therefore, it is likely that there is a large effect on the difference of the local fiber orientation for the initiation of the fatigue crack.

5. CONCLUSIONS

The strength and damage for two kinds of notched FRP specimen — an injection molded specimen and a machined specimen — have been investigated.

For the two kinds of specimen for which both the maximum elastic stress, σ_{max}, and notch-root radius ρ are equal to each other, the strength and the process of damage initiation were similar under static tension.

On the other hand, the number of loading cycles to fatigue damage initiation of the machined specimen were fewer than that of the injection molded specimen.

REFERENCES

1. M. Spearing, P. W. R. Beaumont and M. F. Ashby, Fatigue damage mechanics of notched graphite-epoxy laminates, in: *Composite Materials: Fatigue and Fracture, ASTM STP 1110*, T. K. O'Brien (Ed.), pp. 617–637. ASTM (1991).
2. M.-H. R. Jen, Y. S. Kau and J. M. Hsu, Initiation and propagation of delamination in a centrally notched composite laminate, *J. Compos. Mater.* **27**, 272–302 (1993).
3. S. Ogihara, N. Takeda and A. Kobayashi, Characterization and modeling of fatigue damage in quasi-isotropic CFRP laminates with circular holes by scanning acoustic microscopy, *Adv. Composite Mater.* **6,** 65–73 (1996).
4. T. Ohki, A. Nakai, H. Hamada, N. Takeda and M. Iwamoto, Micro/macro damage evaluation of flat braided composites with a circular hole, in: *Design and Manufacturing of Composites*, S. V. Hoa, H. Hamada, J. Lo and A. Yokoyama (Eds), pp. 75–82 (2000).
5. H. Hyakutake, H. Nisitani and T. Hagio, Fracture criterion of notched plates of FRP, *JSME Inter. J.* **32**, 300–306 (1989).
6. H. Hyakutake, T. Hagio and T. Yamamoto, Fatigue failure criterion for notched FRP plates, *JSME Inter. J.* **36**, 215–219 (1993).
7. H. Hyakutake, Fracture criterion for notched bars of rigid plastics and FRP, *Materials System* **11**, 33–42 (1992).
8. H. Hyakutake and T. Yamamoto, Evaluation of damage of notched FRP plates in static load, *Sci. Engng Compos. Mater.* **6**, 121–129 (1997).
9. H. Hyakutake and T. Yamamoto, Effect of notch geometry on the fatigue damage of glass fiber-reinforced polycarbonate, in: *Proc. 5th Japan Int. SAMPE Symp.*, pp. 119–124 (1997).
10. H. Hyakutake and T. Yamamoto, Luminance decline and microfracture during fatigue loading in notched FRP plates, in: *Experimental Mechanics*, Vol. 2, I. M. Allison (Ed.), pp. 1059–1064. A. A. Balkema, Rotterdam (1998).